Acta Crystallographica Section D
Biological Crystallography
ISSN 0907-4449

Structure of the imipenem-hydrolyzing class A β-lactamase SME-1 from *Serratia marcescens*

Wladimir Sougakoff,[a] Guillaume L'Hermite,[b] Lucile Pernot,[a] Thierry Naas,[c] Valérie Guillet,[d] Patrice Nordmann,[c] Vincent Jarlier[a] and Jean Delettré[e]*

[a]Laboratoire de Recherche Moléculaire sur les Antibiotiques (LRMA), INSERM EMI0004, Faculté de Médecine Pitié-Salpêtrière, Université Pierre et Marie Curie, 75634 Paris CEDEX 13, France, [b]BioXtal, 2 Route de la Noue, 91193 Gif sur Yvette CEDEX, France, [c]Laboratoire de Bactériologie-Virologie, Hôpital de Bicêtre, 94275 Le Kremlin-Bicêtre, France, [d]Groupe de Cristallographie Biologique, Institut de Pharmacologie et de Biologie Structurale, UPR 9062 CNRS, 205 Route de Narbonne, 31077 Toulouse, France, and [e]Laboratoire de Minéralogie-Cristallographie de Paris, CNRS URA 09, Université Paris VI, 4 Place Jussieu, 75252 Paris CEDEX 05, France

Correspondence e-mail: delettre@lmcp.jussieu.fr

Received 27 July 2001
Accepted 15 November 2001

PDB Reference: SME-1, 1dy6.

The structure of the β-lactamase SME-1 from *Serratia marcescens*, a class A enzyme characterized by its significant activity against imipenem, has been determined to 2.13 Å resolution. The overall structure of SME-1 is similar to that of other class A β-lactamases. In the active-site cavity, most of the residues found in SME-1 are conserved among class A β-lactamases, except at positions 104, 105 and 237, where a tyrosine, a histidine and a serine are found, respectively, and at position 238, which is occupied by a cysteine forming a disulfide bridge with the other cysteine residue located at position 69. The crucial role played by this disulfide bridge in SME-1 was confirmed by site-directed mutagenesis of Cys69 to Ala, which resulted in a mutant unable to confer resistance to imipenem and all other β-lactam antibiotics tested. Another striking structural feature found in SME-1 was the short distance separating the side chains of the active serine residue at position 70 and the strictly conserved glutamate at position 166, which is up to 1.4 Å shorter in SME-1 compared with other class A β-lactamases. Consequently, the SME-1 structure cannot accommodate the essential catalytic water molecule found between Ser70 and Glu166 in the other class A β-lactamases described so far, suggesting that a significant conformational change may be necessary in SME-1 to properly position the hydrolytic water molecule involved in the hydrolysis of the acyl-enzyme intermediate.

1. Introduction

β-Lactamases (E.C. 3.5.2.6) catalyse the nucleophilic attack and hydrolysis of the β-lactam ring of β-lactam antibiotics. Based on their sequence homology, β-lactamases have been grouped into four classes (A, B, C and D; Bush *et al.*, 1995; Joris *et al.*, 1991). The class A β-lactamases, which include the TEM and SHV series, are the most frequently encountered enzymes and are characterized by a wide variety of amino-acid sequences and a fairly large diversity of substrate profiles (Bush *et al.*, 1995). Nevertheless, all the class A β-lactamases described so far are characterized by highly conserved residues, including the active-site serine found at position 70, the residues Lys73, Ser130, Asn132, Glu166, Asn170 and the KTG (or KSG) motif found in position 234, which are all involved in the antibiotic binding and/or the two-step mechanism of hydrolysis (acylation–deacylation; Frère *et al.*, 1999; Galleni *et al.*, 1995; Matagne *et al.*, 1998). Of these, the serine residue found at position 70 is generally accepted as playing the role of nucleophile in acylation (Frère *et al.*, 1999). Lys73 would then be involved in both the acylation and deacylation steps of the catalytic mechanism by participating in a proton shuttle in which an H atom is transferred to the lactam nitrogen (Lietz *et al.*, 2000; Matagne *et al.*, 1998). Ser130 has also been suggested

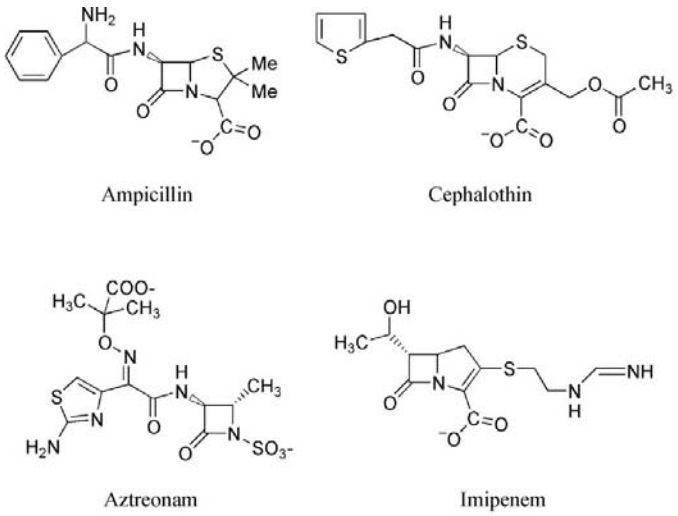

Figure 1
Structures of the four main groups of β-lactam antibiotics: penicillins (ampicillin), cephalosporins (cephalothin), monobactams (aztreonam) and carbapenems (imipenem).

to play a role in the proton transfer and would be activated by the Lys234 residue in the K_{234}-(T/S)-G_{236} element (Matagne *et al.*, 1998). Finally, Glu166 would act as general base, activating Ser70 towards attack on the lactam carbonyl during acylation and promoting a water molecule for hydrolysis of the acyl-enzyme intermediate during deacylation (Matagne *et al.*, 1998).

Imipenem, which belongs to the carbapenem group (Fig. 1), is characterized by a very broad spectrum of activity and is used as a last resort for treating infections caused by multi-resistant organisms. To date, β-lactamase-mediated resistance to imipenem remains infrequent and is mostly associated with production of class B metallo-β-lactamases using an active-site zinc ion to hydrolyse the β-lactam ring (Raquet *et al.*, 1997). However, a subgroup of three well characterized class A enzymes capable of hydrolysing imipenem has been described recently, including NMC-A and IMI-1 from *Enterobacter cloacae* (Naas & Nordmann, 1994) and SME-1 from *S. marcescens* (Naas *et al.*, 1994; Yang *et al.*, 1990). NMC-A, which shares 45% identity with the class A β-lactamase from *Bacillus licheniformis* (Fig. 2), shows strong hydrolytic activity towards imipenem (k_{cat} = 130–1040 s^{-1}; see Table 1). The kinetic parameters of NMC-A also indicate that the enzyme is active against aztreonam and has a low but significant activity towards cefoxitin (Table 1). The crystal structure of NMC-A has been determined, suggesting that the peculiar position of Asn132 in the active site is important for catalytic efficiency against imipenem and cefoxitin (Swaren *et al.*, 1998). Indeed, a significant displacement of Asn132 away from the centre of the catalytic cleft has been observed in NMC-A and would provide additional space in a region where the 6α-hydroxyethyl moiety of imipenem is accommodated. This specific structural organization was suggested to play a major role with respect to the imipenemase activity since it occurs in a critical area for protein–substrate interactions (Swaren *et al.*, 1998).

Table 1
Catalytic parameters determined with SME-1 and NMC-A for various β-lactam antibiotics.

	SME-1†			NMC-A‡		
Antibiotic	k_{cat} (s^{-1})	K_m (μM)	k_{cat}/K_m (mM^{-1} s^{-1})	k_{cat} (s^{-1})	K_m (μM)	k_{cat}/K_m (mM^{-1} s^{-1})
Penicillin G/ amoxicillin§	12	15	800	816	90	9060
Ticarcillin	7	100	70	81	152	530
Cephalothin	50	65	780	2820	185	15200
Aztreonam	80	290	280	707	125	5600
Imipenem	100	230	440	1040	92	11300
Cefoxitin	3	3000	1	5	93	62

† Queenan *et al.* (2000); Raquet *et al.* (1997); Sougakoff *et al.* (1999). ‡ Mariotte-Boyer *et al.* (1996). Kinetic parameters for turnover of imipenem by NMC-A have also been reported by Mourey *et al.* (1998) with the following values: k_{cat} = 130 s^{-1}; K_m = 340 μM; k_{cat}/K_m = 382 mM^{-1} s^{-1}. § Activities determined using penicillin G for SME-1 and amoxicillin for NMC-A.

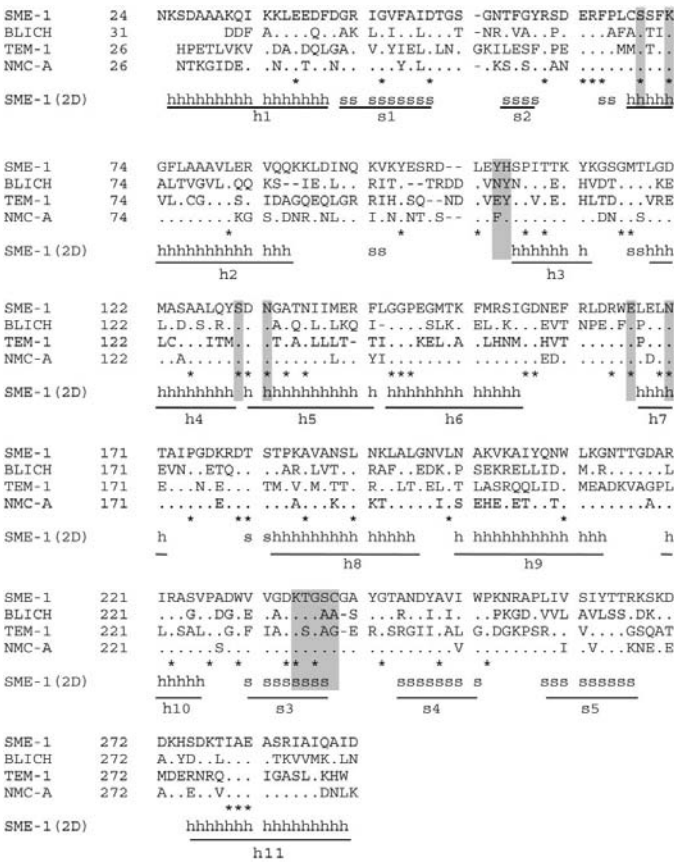

Figure 2
Secondary structure (2D) and multiple sequence alignment of the SME-1 β-lactamase and three class A enzymes, the β-lactamase from *B. licheniformis* (BLICH), TEM-1 and NMC-A. Dashes indicate gaps inserted to optimize the alignment. Dots and stars are used when the sequences in BLICH, TEM-1 and NMC-A are identical to that found in SME-1. Shaded letters show the residues found in the active site. The numbering is that of Ambler *et al.* (1991) and requires (i) that numbers 58 and 254 be deleted in the SME-1 numbering and (ii) that the Phe residue in the sequence FLGGPEGMTK be attributed number 141b. α and β secondary-structure elements are underlined and are indicated by h and s, respectively.

Table 2
Data-collection, data-processing and refinement statistics.

Values in parentheses refer to the highest resolution shell.

Source	Rotating anode
Wavelength (Å)	1.5418
Temperature (K)	291
Resolution range (Å)	20–2.13 (2.28–2.13)
No. of observations	55772 (3390)
No. of unique reflections	24447 (1601)
Data completeness (%)	82 (30.1)
Data redundancy	2.3 (2.1)
R_{sym} (%)	4.9 (21.6)
R_{factor} (%)	18.4
R_{free} (%)	24.4
Average B factor (Å^2)	19.2
R.m.s. bond lengths (Å)	0.007
R.m.s. bond angles (°)	1.440
Solvent atoms	397

The nucleotide sequence of the structural gene encoding SME-1 was reported by Naas *et al.* (1994). At the amino-acid level, the mature protein shares 70% identity with NMC-A and up to 50% with other class A β-lactamases. The kinetic data shown in Table 1 indicate that SME-1 appears to be a less efficient β-lactamase compared with NMC-A. In particular, the hydrolysis rates of SME-1 for imipenem and aztreonam are approximately tenfold lower than those reported for NMC-A by Mariotte-Boyer *et al.* (1996), but it must be noted here that the values of k_{cat} and K_m reported by Mourey *et al.* (1998) for the turnover of imipenem by NMC-A are very similar to those determined from SME-1 (Table 1). On the basis of homology modelling, a structural model of SME-1 was predicted and used to highlight several residues, including Cys69, Ser237 and Cys238, which are potentially involved in its catalytic activity against imipenem (Raquet *et al.*, 1997). According to this model, the two cysteine residues found at positions 69 and 238 would form a disulfide bridge as in NMC-A, which was suggested to be the main factor determining the specific substrate profile of the enzyme (Raquet *et al.*, 1997). More recently, we have used site-directed mutagenesis to construct an SME-1 mutant in which the serine residue found at position 237 has been replaced by an alanine, resulting in a significant decrease in catalytic activity against imipenem (Sougakoff *et al.*, 1999). Such residues were expected from the SME-1 three-dimensional model to contribute to the active-site cavity, but no experimental work was performed to confirm this assumption and compare further the structures of NMC-A and SME-1.

We present here the crystal structure of SME-1, which has been solved by molecular replacement and refined to a resolution of 2.13 Å. The positioning of the potentially important residues previously identified by biochemical and modelling studies was investigated in light of the experimental three-dimensional structure obtained. The critical role played by the disulfide bridge found between Cys69 and Cys238 was demonstrated by replacing the cysteine found in position 69 by an alanine, which is the equivalent amino acid in TEM-1. Finally, comparison of the three-dimensional models for SME-1 and NMC-A reveals significant structural differences in the corresponding catalytic sites.

2. Materials and methods

2.1. Purification and crystallization

SME-1 was expressed, purified and crystallized as previously described (Sougakoff *et al.*, 1996). In brief, crystals were obtained by the hanging-drop vapour-diffusion method using 17% polyethylene glycol 4000 as precipitant in 0.2 *M* ammonium acetate, 0.1 *M* Tris–HCl pH 8.5. The crystals belong to the monoclinic space group $P2_1$, with unit-cell parameters a = 81.50, b = 51.72, c = 71.69 Å, β = 118.62°. The asymmetric unit contains two SME-1 molecules.

2.2. Data collection

As previously reported (Sougakoff *et al.*, 1996), a 2.13 Å data set was collected at 291 K from a single crystal on a Nonius FAST area detector with Cu $K\alpha$ X-rays generated from a rotating anode operated at 70 mA and 40 kV (Sougakoff *et al.*, 1996). Data were collected using 0.1° oscillations and a crystal-to-detector distance of 70 mm. X-ray diffraction data were processed with *MADNES* (Messerschmidt & Pflugrath, 1987) and *AGROVATA* from the *CCP*4 software package (Collaborative Computational Project, Number 4, 1994). The data set was 94% complete to 2.28 Å resolution (82% to 2.13 Å), with 24 447 unique reflections. Other data-collection statistics are given in Table 2.

2.3. Molecular replacement

The crystal structure of SME-1 was solved by molecular replacement with *AMoRe* (Navaza, 1994) using the coordinates of NMC-A as a search model (PDB code 1bul; Swaren *et al.*, 1998) with data in the resolution range 10–2.13 Å. Since the sequences of NMC-A and SME-1 share 70% identity, the search model included the side chains of all of the conserved residues, with alanine substituted at the positions of the non-conserved residues. All calculations were carried out using the *CCP*4 software package.

2.4. Crystallographic refinement

Crystallographic refinement and model building were performed using alternating cycles of *X-PLOR* refinement (Brünger *et al.*, 1987) and manual fitting of the model to the electron density using the program *O* (Jones *et al.*, 1991). The molecular-replacement model was used as a starting model. During the course of refinement, strict NCS (non-crystallographic symmetry) restraints were applied, except for the final cycles, during which the two molecules were refined independently. Refinement converged at an R factor of 18.4% and a free R factor of 24.4% calculated from 10% of the reflections. The final model comprised residues Asn24–Asp291 of molecules A and B and 397 water molecules. Refinement statistics are summarized in Table 2. The geometric parameters of the model were analysed with *PROCHECK* (Laskowski *et al.*, 1993).

2.5. Site-directed mutagenesis.

Plasmid pPTN121, which contains the entire gene coding for SME-1, has been described previously (Naas *et al.*, 1994). The mutation was generated by site-directed mutagenesis using the Muta-Gene M13 *in vitro* mutagenesis kit (Bio-Rad, France). After site-directed mutagenesis, the recombinant plasmid encoding the mutant enzyme, pPTN69A, was introduced by transformation into *Escherichia coli* JM109 (Promega, USA). The mutant gene was sequenced entirely on both strands using an ABI 311 DNA sequencer (Applied Biosystem, France). The sequences of the oligonucleotides used in this study are available upon request. Other standard recombinant DNA methods were carried out according to Sambrook *et al.* (1989). The antibiotic susceptibility profiles of the *E. coli* JM109 strains producing SME-1 or the mutant enzyme were determined by the disc diffusion method using Mueller–Hinton agar plates, as previously described (Barnaud *et al.*, 1998).

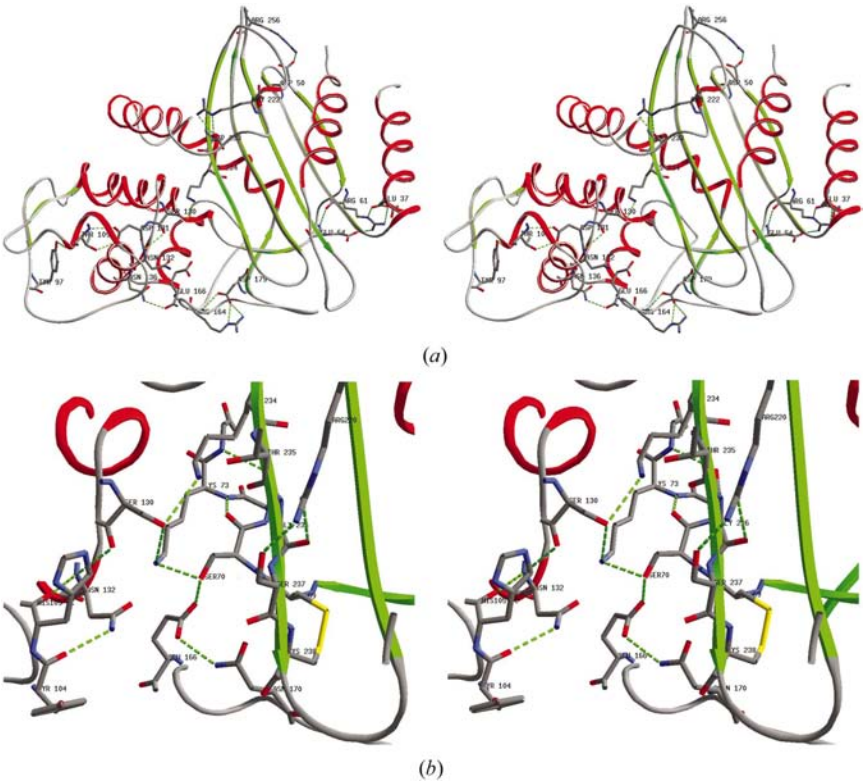

Figure 3
(*a*) Stereoview of the ribbon diagram of the SME-1 β-lactamase. The helices are coloured red and the β-sheets are green. The conserved amino-acid residues interacting with one another in the tertiary structure by hydrogen bonds or salt-bridge interactions are also represented. Dashed lines indicate the hydrogen-bonding interactions. (*b*) Stereoview of the active-site region in SME-1: α-helices are in red, β-strands in green. Hydrogen bonds are depicted by green dotted lines. The disulfide bridge between Cys69 and Cys238 is indicated in yellow. O atoms are coloured red, C atoms grey and N atoms blue.

3. Results

3.1. Structure determination

SME-1 crystallized from polyethylene glycol at pH 8.5 in space group $P2_1$, with two molecules in the asymmetric unit (Sougakoff *et al.*, 1996). The three-dimensional structure of SME-1 was solved by molecular replacement using the coordinates of NMC-A as a search model (Swaren *et al.*, 1998). Molecular replacement was carried out considering two molecules in the asymmetric unit. The self-rotation function showed no peaks except that at the origin, while the cross-rotation function showed a single peak at $\alpha = 159.6$, $\beta = 10.94$, $\gamma = 318.45^\circ$. Using this orientation, we searched for a translation peak, which was initially found at $x = 0.41$, $y = 0$ and $z = 0.148$. However, this solution led to a model that did not refine well and could not account for additional electron density observed after refinement. Therefore, we searched for another translation peak and the solution with $x = 0.80$, $y = 0.951$, $z = 0.613$ was finally considered. According to this solution, the two SME-1 molecules, which were designated *A* and *B*, were related to each other through a pseudo-binary screw axis almost parallel to the 2_1 axis. The individual parameters for each monomer after refinement were molA, $\alpha = 153.61$, $\beta = 9.54$, $\gamma = 325^\circ$, $x = 0.409$, $y = 0$, $z = 0.148$, and molB, $\alpha = 164.68$, $\beta = 18.87$, $\gamma = 313.19^\circ$, $x = 0.878$, $y = 0.951$, $z = 0.614$, with a correlation coefficient of 73.4% and a crystallographic *R* factor of 32.2%. The electron-density map calculated from the dimeric solution was of good quality and was complete along the polypeptide chain, except for the two N-terminal amino-acid residues Asn24 and Lys25 (Ambler's numbering scheme; Ambler *et al.*, 1991). After refinement, the final crystallographic *R* factor was 18.4% at 2.13 Å resolution. The other statistics for the final model of SME-1 are presented in Table 2. The model comprised residues 24–291 of molecules *A* and *B*, *i.e.* the complete mature protein. The Ramachandran plot (data not shown) was consistent with a well defined structure. However, Asn24 and Lys25 exhibited elevated temperature factors and no electron density was associated with the side chains of these two residues. 397 water molecules were refined with the protein structure. It must be noted here that a strong density peak was observed in the active-site cavity of each monomer. After refinement, the peak appeared to be a cluster of two peaks which was finally interpreted as a group of two water molecules bound in the active site (HOH-111 and HOH-186 in molecule *A* and HOH-89 and HOH-143 in molecule *B*). The secondary-structure analysis with *PROCHECK* (Laskowski *et al.*, 1993) indicated that 91.5% of the residues were in most favoured regions, 7.7% in additionally allowed regions and 0.9% in generously allowed regions. Among the latter, residue Phe40 was in an unfavourable conformation because of a strained main-chain geometry. It can be noted here that the electron density observed in position 241 after refinement indicated the

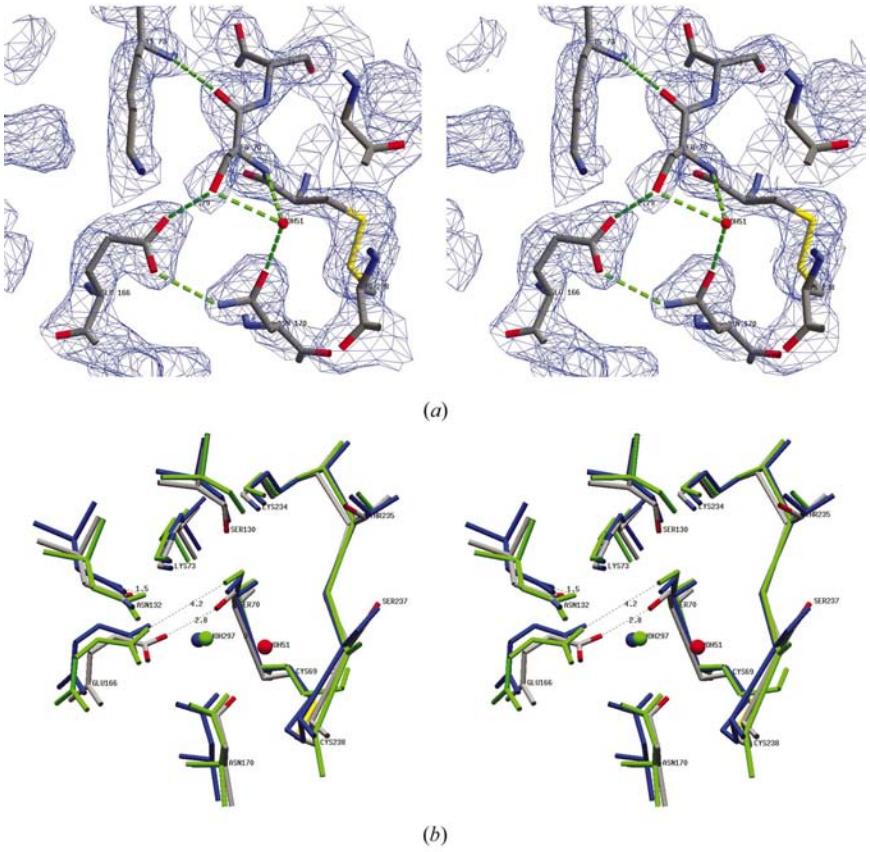

Figure 4
(*a*) Stereoview of the $2F_o - F_c$ electron density (contour level 1σ) around the active site of SME-1. The water molecule in the oxyanion hole (HOH51) is represented by a red sphere. (*b*) Superimposition of SME-1 (CPK colours), TEM-1 (coloured green; PDB code 1btl) and NMC-A (coloured blue; PDB code 1bul). Water molecules are represented by spheres (green for TEM-1, blue for NMC-A and red for SME-1). The distances are given in Å.

presence of a tyrosine residue instead of the isoleucine reported in the previously published sequence (Naas *et al.*, 1994). To confirm the presence of Tyr241 in SME-1, we sequenced the $bla_{\text{SME-1}}$ gene from pPTN121. Analysis of the so deduced amino-acid sequence confirmed that there is a tyrosine at position 241 in SME-1.

3.2. Overall structure

Like all the other class A β-lactamases described so far (Dideberg *et al.*, 1987; Herzberg & Moult, 1987; Ibuka *et al.*, 1999; Joris *et al.*, 1991; Knox & Moews, 1991; Strynadka *et al.*, 1992; Swaren *et al.*, 1998), the polypeptide chain of SME-1 folds into two distinct domains divided by a cleft, with a typical α/β structural organization (Fig. 3*a*). When compared with one another, the two SME-1 molecules found in the asymmetric unit showed very similar conformations: the r.m.s.d. (root-mean-square deviation) of C^{α} positions was 0.16 Å, the largest differences found between the two molecules all being located in loops establishing intermolecular contacts in the crystal (data not shown). The structure includes 11 α-helices (h1–h11; see Fig. 2) and five β-strands (s1–s5) forming the β-sheet in the α/β domain (Fig. 3*a*). Note here that some of these secondary structural elements are linked to each other in the structure by salt bridges or hydrogen bonds formed between amino-acid residues highly conserved among the sequences of SME-1, NMC-A, TEM-1 and the enzyme from *B. licheniformis*. As shown in Fig. 3(*a*), the conserved residue Tyr97 interacts with Thr109 on helix h3, stabilizing the large loop connecting h2 to h3. The side chain of the latter residue is also hydrogen bonded to Asp131 on the h4–h5 loop, whereas the neighbouring residue Ser130 located at the C-terminal part of helix h4 interacts through a hydrogen bond with the side chain of Lys234 found on strand s3. The other conserved residues which seem to play a role in the stabilization of the folding of SME-1 are Glu37 and Arg61 (salt bridge between h1 and s2), Asp50 (strand s1) which forms a salt bridge with Arg256 in the loop connecting s4 to s5, Asn136 and Glu166 (hydrogen-bonding interactions between h5 and the so-called ω-loop structure), Arg164 and Asp179 (salt bridge stabilizing the ω loop), and Arg222 and Asp233 (salt bridge between h10 and s3) (Fig. 3*a*).

Compared with other class A β-lactamases, the overall C^{α} structure of SME-1 can be easily superimposed on that of NMC-A from *Enterobacter cloacae* (r.m.s.d. = 0.46 Å; Swaren *et al.*, 1998), of TEM-1 (r.m.s.d. = 1.19 Å; Jelsch *et al.*, 1993) and with the β-lactamase from *B. licheniformis* (r.m.s.d. = 1.06 Å; Knox & Moews, 1991). As in NMC-A (Swaren *et al.*, 1998), the SME-1 protein fold appears to be stabilized by the disulfide bond formed between the two cysteine residues found at positions 69 and 238 (Fig. 3*b*). Another particular element in SME-1, which was also reported for the β-lactamase from *Staphylococcus aureus* PCI (PDB code 3blm; Herzberg, 1991), is the *cis*-leucine found at position 167 (data not shown), which is stabilized by the hydrogen-bonding interaction between the main-chain carbonyl group of Glu166 and the side chain of Asn136 (Fig. 3*a*).

3.3. The SME-1 active site

Fig. 3(*b*) depicts the amino-acid residues and hydrogen-bonding network in the active site of SME-1. The binding cavity contains most of the conserved residues that are generally accepted as playing an important role in substrate binding and/or catalysis, *i.e.* the active-site serine at position 70, Lys73, Ser130, Asn132, Glu166, Asn170, Arg220, Lys234, Thr235 and Gly236. As previously reported for other enzymes (Jelsch *et al.*, 1993), a dense network of hydrogen bonds connects most of these residues with one another. As shown in

Fig. 3(*b*), the side chain of Lys73 makes hydrogen bonds with the hydroxyl groups of Ser70 and Ser130. Unexpectedly, the relative location of Ser70 and the strictly conserved glutamate residue located at position 166 was found to be significantly different in SME-1 compared with the other class A β-lactamases. Indeed, the Ser70–Glu166 distance in the SME-1 active-site cavity is 2.8 Å, so that the hydroxyl moiety of Ser70 is involved in direct hydrogen bonding to the carboxyl group of Glu166 (Fig. 4*a*). Consequently, when the three-dimensional structure of SME-1 is superimposed onto TEM-1 and NMC-A, the main difference between the three models is found at the level of Ser70 and Glu166, the distance between the corresponding side chains being 4.2 Å in TEM-1 and 3.9 Å in NMC-A as opposed to 2.8 Å in SME-1 (Fig. 4*b*). Because of the steric hindrance created by this peculiar positioning, the catalytic water molecule usually found between Ser70, Glu166 and Asn170 in class A β-lactamases (HOH-297 in TEM-1; Fig. 4*b*) cannot be accommodated in SME-1. It must be mentioned here that a water molecule, HOH-51, is found in the active site of SME-1 (Fig. 4*a*). This water molecule hydrogen bonds to the side chain of Asn170 and to the main-chain nitrogen group of Ser70, one of the two N atoms forming the oxianion hole in class A β-lactamases (Jelsch *et al.*, 1993; Strynadka *et al.*, 1992). Therefore, it would correspond in TEM-1 to the water molecule occupying the oxianion hole in absence of substrate (Jelsch *et al.*, 1993).

Asn132 is an amino-acid residue that is of special interest in class A carbapenemases. The position of this residue was previously found to be unusual in the carbapenemase NMC-A, in which it is displaced by 1.5 Å compared with the TEM-1 enzyme (Fig. 4*b*). This structural feature was suggested to provide critical additional space in NMC-A in the region of the active site where imipenem is accommodated (Swaren *et al.*, 1998). Strikingly, Asn132 occupies a position in SME-1 that is almost identical to that observed in the penicillinase TEM-1 (Fig. 4*b*).

The serine residue found at position 237 in SME-1, which has previously been shown to contribute to the imipenemase activity of this enzyme (Sougakoff *et al.*, 1999), appears to occupy a solvent-exposed position, with its side-chain OH group making a hydrogen-bonding interaction with the guanidinium group of Arg220 (Fig. 3*b*). On the opposite side of the active-site cleft are two residues, Tyr104 and His105, which are conserved in the carbapenem-hydrolysing class A β-lactamases. The bulky side chain of Tyr104 points away from the protein toward the solvent, whereas that of His105 faces the s3 strand in a region involved in the binding of the antibiotic (Fig. 3*b*).

One of the other major differences observed in SME-1 compared with TEM-1 concerns positions 69 and 238. As mentioned above, these positions in SME-1 are occupied by two cysteine residues forming a disulfide bridge also found in the other class A carbapenem-hydrolysing enzyme NMC-A (Swaren *et al.*, 1998). The presence of the 69–238 disulfide bridge in SME-1 seems to have two structural consequences in the binding cavity. First, it could contribute to fixing the position of Ser70 relative to that of the s3 strand (encompassing residues Lys234 to Cys238) by making a covalent link between positions 69 and 238 in the active site (Figs. 3*b* and 4*a*). Secondly, it reorients the main-chain carbonyl O atom in position 238 toward the active-site cavity (Fig. 4*a*), as previously shown in NMC-A (Swaren *et al.*, 1998). To determine whether the 69–238 disulfide bridge in SME-1 is required for the β-lactamase activity of this enzyme, a mutant protein in which Cys69 was substituted by Ala was produced. The antibiotic susceptibility profiles of the *E. coli* strains producing the wild-type and the mutant enzymes were determined, showing that the strain producing the Cys69Ala mutant was fully susceptible to imipenem and to all of the other β-lactam antibiotics tested (Fig. 5).

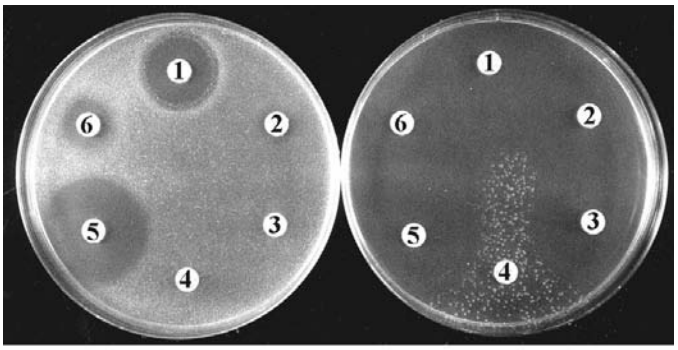

Figure 5
Antibiotic susceptibility testing of *E. coli* producing SME-1 (*a*) and the C69A mutant (*b*). The antibiotics used were imipenem (1), amoxicillin (2), ticarcillin (3), kanamycin (4), cefoxitin (5) and aztreonam (6).

4. Discussion

Analysis of the crystal structure of SME-1 reveals several major structural differences with respect to the other class A enzymes. The most surprising modification is the peculiar relative location of Ser70 and Glu166 in the active-site cleft. The hydroxyl moiety of the former residue is at a hydrogen-bonding distance from the carboxylate group of the latter (2.8 Å), a distance too short to accommodate the catalytic water molecule in a position equivalent to that observed in TEM-1 and NMC-A. In agreement with this, we observed no electron density in SME-1 that could account for the presence of a water molecule between Ser70, Glu166 and Asn170 either in molecule *A* or in molecule *B*. There is a consensus of opinion that Glu166 acts in class A β-lactamases as a general base and activates Ser70 *via* the hydrolytic water molecule embeded between these two residues (Jelsch *et al.*, 1993; Knox & Moews, 1991; Knox *et al.*, 1993; Maveyraud, Pratt *et al.*, 1998; Strynadka *et al.*, 1992; Zawadzke *et al.*, 1996). In SME-1, it is likely that the direct hydrogen-bonding interaction observed between the side chains of Ser70 and Glu166 strongly enhances the nucleophilicity of the hydroxyl group of the serine residue for the initial attack on the carbonyl C atom of the β-lactam ring of imipenem. However, regarding the hypothetical acyl enzyme intermediate obtained, one may wonder how the hydrolytic attack of the acyl group in the

reaction intermediate and the concomitant release of the inactivated antibiotic can occur if a deacylating water molecule is not properly positioned and activated by Glu166. With the water molecules found in the active site of SME-1, it can be hypothesized that HOH-51, which is located in the oxyanion hole of the apoenzyme (see Fig. 4*a*), may be a possible partner in the deacylation step provided that it shifts upon binding of the substrate from its initial location to a proximal position closer to Glu166 where it could be activated for the hydrolytic attack. Considering that the complex formed between SME-1 and the β-lactam antibiotic is not rigid and can probably undergo significant conformational rearrangements upon binding of the substrate (Maveyraud, Mourey *et al.*, 1998; Mourey *et al.*, 1999), there is a cavity between Glu166 and Asn170 in the electron-density map conceivably large enough to accommodate such a water molecule (Fig. 4*a*), but this hypothesis needs to be confirmed by determining the structure of a complex between SME-1 and a β-lactam compound. Finally, it is worth noting here that the low catalytic activity of SME-1 against penicillins, when compared with other class A β-lactamases such as TEM-1 (Matagne *et al.*, 1998), may be linked to the conformational rearrangement required in SME-1 to accommodate the catalytic water molecule in a proper position.

Several other interesting structural features have been observed in SME-1. Firstly, the binding pocket in this enzyme is characterized by the presence of a serine residue in position 237. We recently reported that a Ser237→Ala mutation in SME-1 resulted in a specific fivefold decrease in catalytic activity against imipenem, showing that Ser237 contributes significantly to the imipenemase activity of this enzyme (Sougakoff *et al.*, 1999). The structural analysis reported here is consistent with these results since the main-chain NH group of Ser237, the side chain of which is strongly stabilized by two hydrogen bonds with Arg220, contributes to the SME-1 oxyanion hole together with Ser70 (Fig. 3*b*).

Another striking structural element in SME-1 is the disulfide bridge that links Cys69 and Cys238 and which has been described also in the imipenem-hydrolysing enzyme NMC-A (Swaren *et al.*, 1998). It has been previously hypothesized that the presence of this disulfide bridge contributes to the activity of SME-1 against imipenem (Raquet *et al.*, 1997; Swaren *et al.*, 1998). Using site-directed mutagenesis, we have shown that the mutational replacement Cys69→Ala results in an enzyme unable to confer resistance to β-lactam antibiotics, including imipenem. However, the molecular mechanism by which the mutation disrupting the disulfide bridge significantly affects the β-lactamase activity of SME-1 remains to be elucidated (modification of the structural organization of the enzyme or, alternatively, of the stability of the enzyme).

Finally, it has been previously reported that the class A β-lactamase TEM-1 binds imipenem with high affinity but is inhibited by this antibiotic by forming a stable acyl-enzyme intermediate characterized by a specific conformational organization that accounts for the ability of imipenem to resist hydrolytic deactivation by this enzyme (Maveyraud, Mourey *et al.*, 1998). Therefore, one is tempted to hypothesize that the efficacy of SME-1 in hydrolysing imipenem is conditioned not only at the level of substrate recognition and/or acylation, but also at the level of an efficient deacylation of the acyl-enzyme intermediate. Efforts are currently under way to trap an SME-1–β-lactam complex, which should shed further light on the role of the acyl-enzyme intermediate in the imipenemase activity of SME-1.

We gratefully acknowledge J. P. Samama for the coordinates of NMC-A and J. P. Mornon for his initial encouragement of the X-ray analysis of SME-1. We thank E. Collatz for helpful discussions and A. T. Bouthors and J. P. Lagarde for their excellent technical assistance. This work was supported by the Institut National de la Santé et de la Recherche Médicale (Grant EMI 0004) and by the Ministère de la Recherche (PRFMMIP: 'Réseau de Recherche sur les β-lactamases').

References

Ambler, R. P., Coulson, A. F., Frère, J. M., Ghuysen, J. M., Joris, B., Forsman, M., Levesque, R. C., Tiraby, G. & Waley, S. G. (1991). *Biochem. J.* **276**, 269–272.

Barnaud, G., Arlet, G., Verdet, C., Gaillot, O., Lagrange, P. H. & Philippon, A. (1998). *Antimicrob. Agents Chemother.* **42**, 2352–2358.

Brünger, A. T., Kuriyan, J. & Karplus, M. (1987). *Science*, **235**, 458–460.

Bush, K., Jacoby, G. A. & Medeiros, A. A. (1995). *Antimicrob. Agents Chemother.* **39**, 1211–1233.

Collaborative Computational Project, Number 4 (1994). *Acta Cryst.* D**50**, 760–763.

Dideberg, O., Charlier, P., Wery, J. P., Dehottay, P., Dusart, J., Erpicum, T., Frère, J. M. & Ghuysen, J. M. (1987). *Biochem. J.* **245**, 911–913.

Frère, J. M., Dubus, A., Galleni, M., Matagne, A. & Amicosante, G. (1999). *Biochem. Soc. Trans.* **27**, 58–63.

Galleni, M., Lamotte-Brasseur, J., Raquet, X., Dubus, A., Monnaie, D., Knox, J. R. & Frère, J. M. (1995). *Biochem. Pharmacol.* **49**, 1171–1178.

Herzberg, O. (1991). *J. Mol. Biol.* **217**, 701–719.

Herzberg, O. & Moult, J. (1987). *Science*, **236**, 694–701.

Ibuka, A., Taguchi, A., Ishiguro, M., Fushinobu, S., Ishii, Y., Kamitori, S., Okuyama, K., Yamaguchi, K., Konno, M. & Matsuzawa, H. (1999). *J. Mol. Biol.* **285**, 2079–2087.

Jelsch, C., Mourey, L., Masson, J. M. & Samama, J. P. (1993). *Proteins*, **16**, 364–383.

Jones, T. A., Zou, J.-Y., Cowan, S. W. & Kjeldgaard, M. (1991). *Acta Cryst.* A**47**, 110–119.

Joris, B., Ledent, P., Dideberg, O., Fonze, E., Lamotte-Brasseur, J., Kelly, J. A., Ghuysen, J. M. & Frère, J. M. (1991). *Antimicrob. Agents Chemother.* **35**, 2294–2301.

Knox, J. R. & Moews, P. C. (1991). *J. Mol. Biol.* **220**, 435–455.

Knox, J. R., Moews, P. C., Escobar, W. A. & Fink, A. L. (1993). *Protein Eng.* **6**, 11–18.

Laskowski, R. A., MacArthur, M. W., Moss, D. S. & Thornton, J. M. (1993). *J. Appl. Cryst.* **26**, 283–291.

Lietz, E. J., Truher, H., Kahn, D., Hokenson, M. J. & Fink, A. L. (2000). *Biochemistry*, **39**, 4971–4981.

Mariotte-Boyer, S., Nicolas-Chanoine, M. H. & Labia, R. (1996). *FEMS Microbiol. Lett.* **143**, 29–33.

Matagne, A., Lamotte-Brasseur, J. & Frère, J. M. (1998). *Biochem. J.* **330**, 581–598.

Maveyraud, L., Mourey, L., Kotra, L. P., Pedelacq, J.-D., Guillet, V., Mobashery, S. & Samama, J.-P. (1998). *J. Am. Chem. Soc.* **120**, 9748–9752.
Maveyraud, L., Pratt, R. F. & Samama, J. P. (1998). *Biochemistry*, **37**, 2622–2628.
Messerschmidt, A. & Pflugrath, J. W. (1987). *J. Appl. Cryst.* **20**, 306–315.
Mourey, L., Kotra, L. P., Bellettini, J., Bulychev, A., O'Brien, M., Miller, M. J., Mobashery, S. & Samama, J. P. (1999). *J. Biol. Chem.* **274**, 25260–25265.
Mourey, L., Miyashita, K., Swarén, P., Bulychev, A., Samama, J. P. & Mobashery, S. (1998). *J. Am. Chem. Soc.* **120**, 9382–9383.
Naas, T. & Nordmann, P. (1994). *Proc. Natl Acad. Sci. USA*, **91**, 7693–7697.
Naas, T., Vandel, L., Sougakoff, W., Livermore, D. M. & Nordmann, P. (1994). *Antimicrob. Agents Chemother.* **38**, 1262–1270.
Navaza, J. (1994). *Acta Cryst.* A**50**, 157–63.
Queenan, A. M., Torres-Viera, C., Gold, H. S., Carmeli, Y., Eliopoulos, G. M., Moellering, R. C. Jr, Quinn, J. P., Hindler, J., Medeiros, A. A. & Bush, K. (2000). *Antimicrob. Agents Chemother.* **44**, 3035–3039.
Raquet, X., Lamotte-Brasseur, J., Bouillenne, F. & Frère, J. M. (1997). *Proteins*, **27**, 47–58.
Sambrook, J., Fritsch, E. F. & Maniatis, T. (1989). *Molecular Cloning: A Laboratory Manual*, 2nd ed. Cold Spring Harbor, NY: Cold Spring Harbor Laboratory Press.
Sougakoff, W., Jarlier, V., Delettre, J., Colloc'h, N., L'Hermite, G., Nordmann, P. & Naas, T. (1996). *J. Struct. Biol.* **116**, 313–316.
Sougakoff, W., Naas, T., Nordmann, P., Collatz, E. & Jarlier, V. (1999). *Biochim. Biophys. Acta*, **1433**, 153–158.
Strynadka, N. C., Adachi, H., Jensen, S. E., Johns, K., Sielecki, A., Betzel, C., Sutoh, K. & James, M. N. (1992). *Nature (London)*, **359**, 700–705.
Swaren, P., Maveyraud, L., Raquet, X., Cabantous, S., Duez, C., Pedelacq, J. D., Mariotte-Boyer, S., Mourey, L., Labia, R., Nicolas-Chanoine, M. H., Nordmann, P., Frère, J. M. & Samama, J. P. (1998). *J. Biol. Chem.* **273**, 26714–26721.
Yang, Y. J., Wu, P. J. & Livermore, D. M. (1990). *Antimicrob. Agents Chemother.* **34**, 755–758.
Zawadzke, L. E., Chen, C. C., Banerjee, S., Li, Z., Wasch, S., Kapadia, G., Moult, J. & Herzberg, O. (1996). *Biochemistry*, **35**, 16475–16482.